

Higgs boson \mathcal{CP} -properties of the gluonic contributions in Higgs plus three jet production via gluon fusion at the LHC

Francisco Campanario^{1,2,*} and Michael Kubocz^{3,2,†}

¹*Theory Division, IFIC, University of Valencia-CSIC, E-46100 Paterna, Valencia, Spain*

²*Institute for Theoretical Physics, KIT, 76128 Karlsruhe, Germany.*

³*Institut für Theoretische Teilchenphysik und Kosmologie, RWTH Aachen University, D52056 Aachen, Germany*

In high energy hadronic collisions, a general \mathcal{CP} -violating Higgs boson Φ with accompanying jets can be efficiently produced via gluon fusion, which is mediated by heavy quark loops. In this letter we study the dominant sub-channel $gg \rightarrow \Phi ggg$ of the gluon fusion production process with triple real emission corrections at order α_s^5 . We go beyond the heavy top limit approximation and include the full mass dependence of the top- and bottom-quark contributions. Furthermore, we show within a toy-model scenario that bottom-quark loop contributions in combination with large values of $\tan\beta$ can modify visibly the differential distributions sensitive to \mathcal{CP} -measurements of the Higgs boson particle.

PACS numbers: 12.38.Bx, 13.85.-t, 14.65.Fy, 14.65.Ha, 14.70.Dj, 14.80.Bn

I. INTRODUCTION

Since the discovery of a new bosonic resonance with a mass in the range of 125-126 GeV at the Large Hadron Collider (LHC), the measurement of its properties to validate the Standard Model (SM) Higgs boson hypothesis has become one of the main goals of the scientific community [1–10]. Recent measurements by the ATLAS and CMS collaborations favor a spin-0 Higgs boson with a positive parity [11, 12], a pure \mathcal{CP} -odd scalar Higgs particle was already discarded in previous studies [6] with more than three standard deviations. However, a scalar \mathcal{CP} -violating Higgs boson consisting of a mixed state of \mathcal{CP} -odd and \mathcal{CP} -even couplings to fermions has not still been ruled out. It can be described by the following Lagrangian:

$$\mathcal{L}_{\text{Yukawa}} = \bar{q}(y_q + i\gamma_5 \tilde{y}_q) q \Phi, \quad (1)$$

where Φ denotes a scalar Higgs particle with unconstrained \mathcal{CP} properties via the assignment

$$\Phi = H \cos \alpha + A \sin \alpha, \quad (2)$$

with H and A representing a \mathcal{CP} -even and \mathcal{CP} -odd Higgs bosons, respectively, and α the corresponding mixing angle. Higgs production in association with two jets via gluon fusion is a promising channel in order to measure the \mathcal{CP} -properties of the Higgs particle as well as its coupling to fermions [13, 14]. In general, the production of $\Phi + 2$ jets events leads to a distinctively altered distribution of the azimuthal angle difference between the two jets. The maximum of the distribution is found at $\Delta\phi_{jj} = -\alpha$ and $\Delta\phi_{jj} = -\alpha \pm \pi$, in contrast to a pure

\mathcal{CP} -even Higgs $\Phi = H$ or \mathcal{CP} -odd Higgs $\Phi = A$ [1, 15–18], with maximums situated at $\Delta\phi_{jj} = 0$ ($\pm\pi$) and $\Delta\phi_{jj} = \pm\pi/2$, respectively. Thus, the azimuthal angle distribution of Φjj events production provides valuable information about the mixing nature of the scalar particle.

A relevant aspect of interest is the modification of the azimuthal angle correlation by emission of additional jets, that is, at least by a third jet. Several analyses [19–21] demonstrated that the ϕ_{jj} -correlation survives with minimal modifications after the separation of hard radiation from showering effects with subsequent hadronization. Similar conclusions were obtained by a parton level calculation with NLO corrections [22, 23] to the Higgs plus two jets process in the framework of an effective Lagrangian. In this letter, we analyze whether the presence of additional soft radiation may destroy the characteristic pattern observed in Ref. [18] for Φjj production.

For a Higgs mass lower than the top-quark mass, the total cross section can be determined with a good accuracy via the effective Lagrangian derived from the heavy top limit approximation

$$\mathcal{L}_{\text{eff}} = \frac{y_t}{y_t^{SM}} \cdot \frac{\alpha_s}{12\pi v} \cdot H G_{\mu\nu}^a G^{a\mu\nu} + \frac{\tilde{y}_t}{y_t^{SM}} \cdot \frac{\alpha_s}{8\pi v} \cdot A G_{\mu\nu}^a \tilde{G}^{a\mu\nu}, \quad (3)$$

where $G_{\mu\nu}^a$ represents the gluon field strength and $\tilde{G}^{a\mu\nu} = 1/2 G_{\rho\sigma}^a \epsilon^{\mu\nu\rho\sigma}$ its dual. The validity range of the effective approach has been studied at LO for Φjj production in Ref. [18], and recently for $Hjjj$ production in Ref. [24], for which there are additional NLO results computed within the effective theory [25].

For values of the Higgs transverse momentum larger than twice the top mass, Higgs masses bigger than the top mass and finally in models (e.g. 2HDM, MSSM, etc.) with strong enhancement of bottom-loop contributions by a large ratio of the two vacuum expectation values, $v_u/v_d = \tan\beta$, the effective Lagrangian approximation, Eq. 3, breaks down and leads to unreliable predictions.

* francisco.campanario@ific.uv.es

† kubocz@physik.rwth-aachen.de

Here it is necessary to switch to the full theory with full quark mass dependence in the contributing loops.

In this letter, we provide results for Φjjj going beyond the heavy top approximation, including the full mass dependence of the top- and bottom-quark contributions at LO for the sub-process $gg \rightarrow \Phi ggg$ which is the dominant channel, and hence, an essential piece to compute the real emission contributions for Higgs plus two jets production at NLO via GF within the full theory. This production channel involves the manipulation of massive rank-5 hexagon Feynman diagrams, which are the most complicated topologies appearing in Higgs production in association with three jets via GF, and thus it provides a testing ground to check the numerical stability of the full process. This is particularly important for the numerically challenging bottom-loop corrections, which turn out to provide the main contributions at large values of $\tan\beta$, and hence, dominate over the top-loop contributions. Results for the full process and a detailed description of de-correlation effects will be given in a forthcoming publication.

This letter is organized as follows. The technical details of our implementation are presented in Section II. Numerical results are shown in Section III and finally conclusions in Section IV.

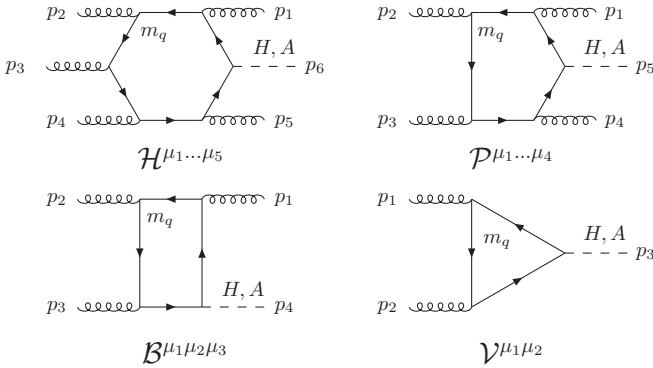


FIG. 1: Master Feynman diagrams

II. CALCULATIONAL DETAILS

The relevant subprocesses contributing to Φjjj production are,

$$\begin{aligned} qq &\rightarrow qqg\Phi, & qQ &\rightarrow qQg\Phi, \\ qq &\rightarrow qqg\Phi, & gg &\rightarrow ggg\Phi. \end{aligned} \quad (4)$$

In this letter, we restrict our study to the last subprocess. In a 2HDM, Yukawa couplings to up- and down-type quarks are generally functions of the ratio of two vacuum expectation values, $\tan\beta = v_u/v_d$. In the scenario of the 2HDM model of type II, the Yukawa coupling to up-type quarks is suppressed by $\cot\beta$ in contrary to

the enhancement by $\tan\beta$ of the Yukawa couplings to down-type quarks,

$$\tilde{y}_u^{\text{II}} = -\frac{\cot\beta}{v}m_u \quad \text{and} \quad \tilde{y}_d^{\text{II}} = -\frac{\tan\beta}{v}m_d. \quad (5)$$

Due to this enhancement, loops with bottom-quarks can also provide significant contributions to the total cross section as well as to differential distributions of important observables. Thus, we take bottom-loop corrections into account to study their phenomenological effects and numerical behavior. In this connection we closely follow the setup described in Ref. [24] for $Hjjj$ production. The here analyzed Higgs production process is available in the GGFLO MC program, which is also a part of the VBFNLO framework [26]. As customary in VBFNLO calculations, we use the effective current approach [27, 28] to evaluate loop amplitudes. Eight master Feynman diagrams involving four \mathcal{CP} -even and four \mathcal{CP} -odd Higgs couplings to fermions are needed. For this letter, the four \mathcal{CP} -odd Higgs master integrals depicted in Fig. 1 have been computed with the in-house framework described in Ref. [29]—the attached gluons are considered to be off-shell vector currents, which allow the attachment of further participating gluons. The numerical evaluation of the tensor integrals follows the Passarino-Veltman approach of Ref. [30] up to boxes, and Ref. [31], with the scheme laid out in Ref. [29], for pentagons and hexagons. Scalar integrals are computed following Refs. [32, 33]. Furthermore, the number of diagrams to be evaluated are reduced by a factor two applying Furrry's theorem. The color factors are the same as for $Hjjj$ production and were computed by hand and cross checked with the program MADGRAPH [34, 35].

To guarantee the correctness of the results, we compare first the amplitudes of the \mathcal{CP} -odd and \mathcal{CP} -even production modes obtained by MADGRAPH in the top limit approximation against a self-made implementation of the Φjjj production channel, implemented also in VBFNLO. The agreement for both the \mathcal{CP} -odd and \mathcal{CP} -even production modes is satisfied at the machine precision level at the amplitude level and at the per mille level when compared at the integrated cross section level against MADGRAPH. Then, we compare the full and effective theory results at the integrated cross section level for $m_t = 5 \cdot 10^4$ GeV. The agreement is better than one per ten thousand level.

To control the numerical instabilities inherent to a multi-leg calculation, we follow the procedure described in Ref. [24]. We provide a summary here for the sake of being self contained. We use the Ward identities technique developed in Ref. [29] and applied successfully in other complex GF processes [24, 36]. These identities allow to relate N -point to $N-1$ -point tensor integrals by replacing an effective current by the corresponding momentum flow. This property is transferred to the Master

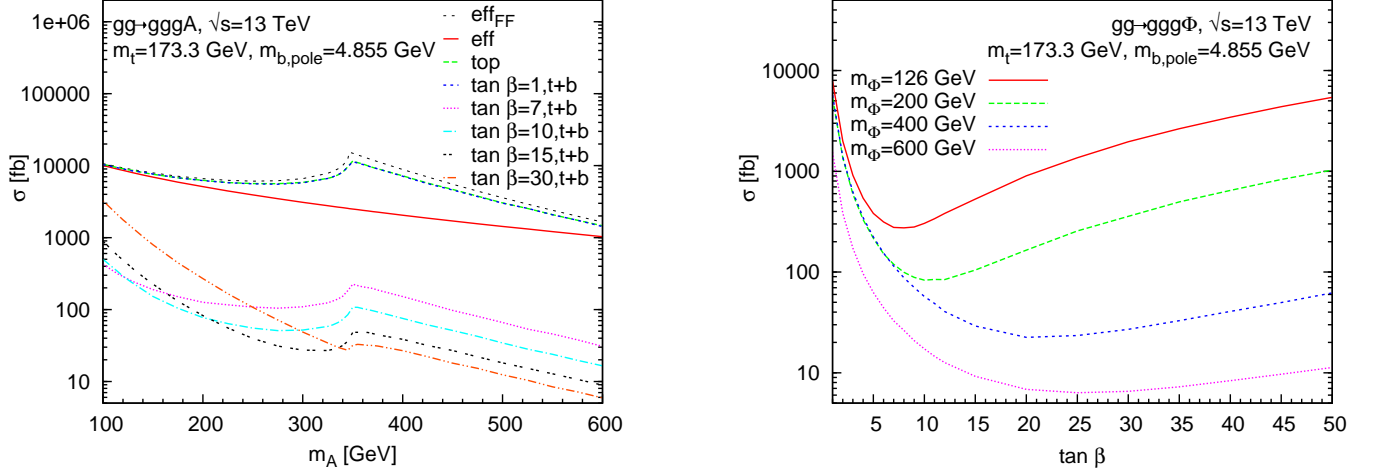


FIG. 2: Left: A + 3 jet cross section as a function of the pseudo-scalar Higgs boson mass, m_A , for different values of $\tan\beta$. Right: Φ + 3 jet cross section as a function of $\tan\beta$ for several values of the Φ mass. The inclusive cuts (IC) of Eq. (7) are applied

integrals, hence it provides a strong check on the correctness of the Master integrals. For example, a hexagon topology of tensor rank five can be written with the help of the Ward identity as a difference of two pentagons topologies of tensor rank four

$$\mathcal{H}^{\mu_1 \dots \mu_5} p_{i, \mu_i} = \mathcal{P}_1^{\mu_1 \dots \hat{\mu}_i \dots \mu_5} - \mathcal{P}_2^{\mu_1 \dots \hat{\mu}_i \dots \mu_5}, \quad i = 1 \dots 5, \quad (6)$$

where $\hat{\mu}_i$ denotes the corresponding vertex replaced by its momentum p_i . We construct all possible Ward identities for each physical permutation and diagram, e.g. all five different ones for the hexagon $\mathcal{H}^{\mu_1 \dots \mu_5}$.

For each phase space point and diagram, these Ward identities are evaluated with a small additional computing effort using a cache system. We request a global accuracy of $\epsilon = 5 \times 10^{-4}$ and reevaluate the diagram using quadruple precision if the Ward Identities are not satisfied with the demanded accuracy. Finally, the amplitude is set to zero and the phase-space point discarded if the Ward identities are not satisfied after this step. The amount of phase-space points, which does not pass the Ward identities after this step is statistically negligible and well below the per mille level.

With this method, we obtain statistical error of 1% in 3 hours (top contributions only) for the LO inclusive cross section using a single core of an Intel i7-3970X processor with the Intel-ift compiler (version 12.1.0). The distributions shown below are based on multiprocessor runs with a total statistical error of up to 0.02%. These precision and computing-time results set a benchmark for comparisons with automated multi-leg calculation programs.

III. NUMERICAL RESULTS

In this section, we present results for integrated cross sections and selected differential distributions of important observables for the sub-process $gg \rightarrow ggg\Phi$ at the LHC at 13 TeV center of mass (c.m.) energy. We use the CTEQ6L1 parton distribution functions (PDFs) [37] with the default strong coupling value $\alpha_s(M_Z) = 0.130$ and the k_T -jet algorithm. To avoid soft and collinear QCD singularities, we introduce a minimal set of cuts:

$$p_T^{j_i} > 20 \text{ GeV}, \quad |y_j| < 4.5, \quad R_{jj} > 0.6, \quad (7)$$

where R_{jj} describes the separation of the two partons in the rapidity versus azimuthal-angle plane,

$$R_{jj} = \sqrt{\Delta y_{jj}^2 + \phi_{jj}^2}, \quad (8)$$

with $\Delta y_{jj} = |y_{j1} - y_{j2}|$ and $\phi_{jj} = \phi_{j1} - \phi_{j2}$. These cuts anticipate LHC detector capabilities and jet finding algorithms and will be called “inclusive cuts” (IC) in the following.

All quarks, except the bottom- and the top-quark are considered massless. The top-quark mass is fixed at $m_t = 173.3$ GeV and $\overline{\text{MS}}$ bottom-quark mass at $\overline{m}_b(m_b) = 4.2$ GeV. In our setup Yukawa couplings contain a 33-42% smaller m_b than the pole mass of 4.855 GeV utilized in the loop propagators within the Higgs-mass range of 100-600 GeV. Although we present a LO calculation, we have taken into account the evolution of m_b up to a reference scale (in this case m_H) due to the dominance of the bottom loop contributions at large values of $\tan\beta$. We achieved this by utilizing the relation between the pole mass and the $\overline{\text{MS}}$ mass, following Refs. [38, 39] within a 5-flavor scheme. The Higgs boson is produced on-shell and without finite width effects. Additionally,

we choose $M_Z = 91.188 \text{ GeV}$, $M_W = 80.386 \text{ GeV}$ and $G_F = 1.16637 \times 10^{-5} \text{ GeV}^{-2}$ as electroweak input parameters and use Standard Model tree level relations to compute the weak mixing angle and the electromagnetic coupling constant.

The factorization scale is set to $\mu_F = (p_T^{j1} p_T^{j2} p_T^{j3})^{1/3}$ and the renormalization to

$$\alpha_s^5(\mu_R) = \alpha_s(p_T^{j1}) \alpha_s(p_T^{j2}) \alpha_s(p_T^{j3}) \alpha_s(p_\Phi)^2. \quad (9)$$

Here, p_T^i with $i = 1, 2, 3$ denotes jets with decreasing transverse momenta.

In the following, if not stated otherwise, we simulate effects of a general \mathcal{CP} -violating Higgs boson, Φ , using a toy model. In general, the Agg coupling is enhanced in comparison to the Hgg one by factor $3/2$ due to loop effects (see Lagrangian of Eq. 3). Although, in our MC program, it is possible to modify arbitrarily the strength of Yukawa couplings being important for general studies, in the considered model, we impose an equal coupling strength to fermions for both, the \mathcal{CP} -even and the \mathcal{CP} -odd parts of Φ . To achieve this, it is necessary to reduce the strength of the \mathcal{CP} -odd coupling by a factor of $2/3$ with respect to Eq. (5):

$$y_d = \frac{3}{2} \tilde{y}_d = -\frac{m_d}{v} \tan \beta \quad \text{and} \quad y_u = \frac{3}{2} \tilde{y}_u = -\frac{m_u}{v} \cot \beta. \quad (10)$$

This set up, as we will see below, will produce a known behavior in the differential distributions sensitive to \mathcal{CP} -Higgs measurements. The left panel of Figure 2 shows for different values of $\tan \beta$ the total cross section of a pure \mathcal{CP} -odd Higgs boson as a function of its mass. One can observe that amplitudes containing both, top and bottom loop corrections, denoted by “t+b” in the following, are indistinguishable from the pure top loop contributions for $\tan \beta = 1$. Both of them demonstrate visibly the expected threshold enhancement at a Higgs mass value corresponding to twice of the top mass. In the case of bottom-quark loop dominated processes, the characteristic peak appears well below the shown Higgs mass range. We also show results for the effective theory approximation with and without applying corrections to the couplings by an additional form factor (FF), obtained from Eq. (2.26) of Ref. [3].

Within a 10% deviation with respect to the full theory, the effective theory gives accurate predictions up to Higgs masses of 150 GeV.

With the help of the form factor FF, similarly applied in the purely \mathcal{CP} -even Higgs boson case of Ref. [24], the validity range is extended up to Higgs masses of about 300 GeV within a 10% deviation. Additionally, it introduces back the threshold behavior at $m_A = 2m_t$. Beyond that validity bound, the total cross section is overestimated up to 20% at $m_H = 370 \text{ GeV}$, and converges afterwards slowly to the full theory result for the shown Higgs mass range. Although, the form factor predicts the normalization of the cross section for $\tan \beta = 1$ relatively

well, large deviations can be still observed in differential distributions, see Ref. [24].

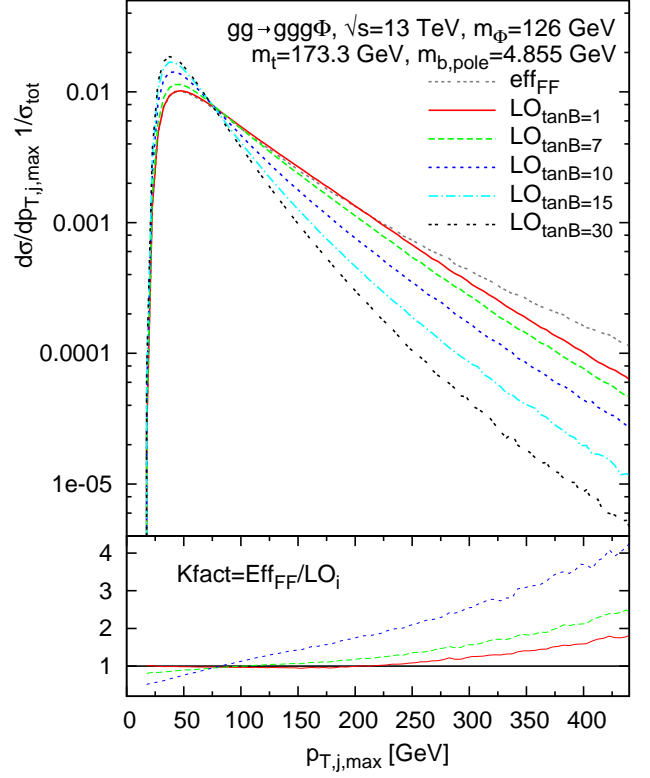


FIG. 3: Transverse-momentum distributions of the harder jet generated within our toy-model scenario including top and bottom loop-induced amplitudes for different values of $\tan \beta$ and for the effective theory with form factors (eff_{FF}). The lower panel shows the ratios of the effective Lagrangian approach vs. the full theory for various $\tan \beta$ values. The inclusive cuts (IC) of Eq. (7) are applied.

In the right panel of Figure 2, we show the total cross section of the production of Φjjj as a function of the parameter $\tan \beta$ computed within our toy-model scenario for different Higgs mass values. Similarly to Φjj production process [18], the minimal cross section for small Higgs masses is obtained near $\tan \beta \approx 7$, when $y_t \approx y_b$ (see Eq. (5)) and both Yukawa couplings are suppressed simultaneously in comparison to y^{SM} . The shift of the minimum of σ to larger $\tan \beta$ values with increasing m_Φ can be understood in the following way: For large values of $\tan \beta$, e.g. $\tan \beta = 30$, illustrated in the left panel of Fig. 2, the bottom-loop contributions dominate over the suppressed top-quark contributions. However, the total cross section decreases rapidly with rising m_Φ values since the scale in the loops is now set by the heavy

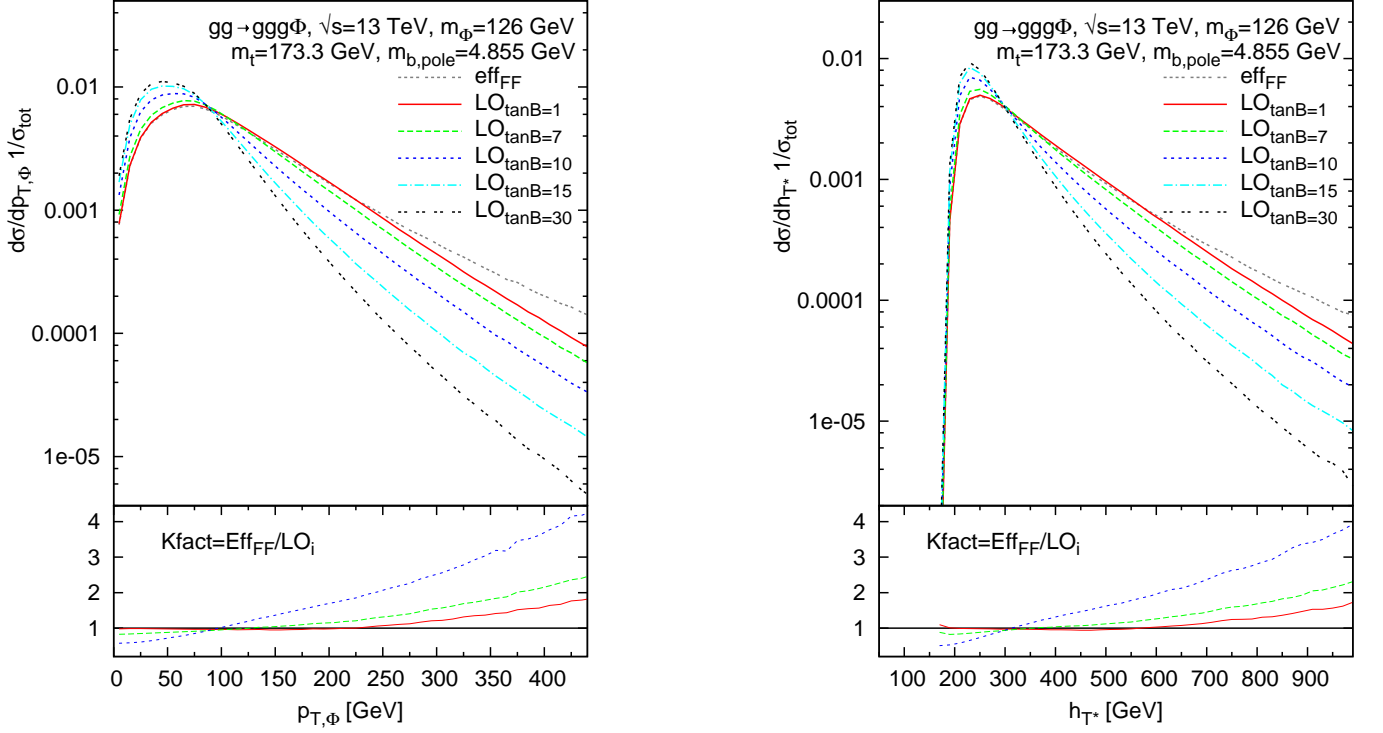


FIG. 4: The transverse-momentum distributions of the Higgs boson Φ (left panel) and the transverse scalar sum (right panel), are plotted. Details are described in Fig. 3 and in the text.

Higgs mass instead of the (relatively) lighter quark mass. The suppression of bottom-loops at large m_Φ implies the equality of the top- and bottom-quark contributions, and therefore as a consequence it leads to a shifted minimum of the distribution towards larger values of $\tan\beta$.

In the following, for a set of different $\tan\beta$ values, we simulate effects of a general \mathcal{CP} -violating Higgs sector at the LHC using the previously described toy model scenario and show differential distributions for several phenomenologically interesting observables for Φjjj production with a Higgs mass fixed at 126 GeV. Fig. 3 shows the differential distribution of the hardest jet. For large values of $\tan\beta$, bottom loop corrections dominate, and hence, provide a strong impact on the spectrum. For $p_{T,j} > m_b$, the large scale of the kinematic invariants leads to an additional suppression of bottom-loop induced sub-amplitudes compared to the heavy quark effective theory. It is e.g. clearly visible for $\tan\beta = 10$ at 400 GeV, where Kfact (lower panel) shows a 4-times overestimated prediction of the heavy theory approach. For $\tan\beta = 1$, the effective theory approximation describes efficiently the full theory prediction within 10% accuracy up to $p_T^{j,\text{max}} < 200$ GeV. Beyond that regime, differences start to increase and deviations up to 100% are found. Hence, these facts stress the limited predictive power of the heavy-top quark limit approximation in scenarios beyond the SM. Similar properties are found in Fig. 4, where the left panel illustrates the differential distribution of the transverse Higgs boson momentum.

The right panel shows the transverse scalar sum of the system, oftenly used in the framework of new physics searches, defined as $H_T = \sum_i p_T^{j_i} + \sqrt{p_{T,\Phi}^2 + M_\Phi^2}$.

The azimuthal angle distribution is sensitive to the \mathcal{CP} -character of the Higgs coupling to fermions. In Ref. [18], it was proven for Φjj production that the softening effects observed in the transverse momentum distributions due to bottom-loop corrections did not modify the jet azimuthal angle correlations predicted by the effective theory approximation. In this letter, the presence of the additional third jet rises the question whether soft radiation can distort these predictions. We follow the definition of Ref. [15] of the azimuthal angle distribution between the more forward and the more backward of the two tagging jets. To increase the sensitivity to the \mathcal{CP} -structure of the Higgs couplings, a modification of the inclusive set of cuts is applied,

$$p_T^{j_i} > 30 \text{ GeV}, |\eta_j| < 4.5, R_{jj} > 0.6, \Delta\eta_{jj} > 3. \quad (11)$$

We refer to them as ICphi set of cuts in the following. The effective theory approach showed a phase shift of the ϕ_{jj} distribution by an angle α which is given by the relative strength of the \mathcal{CP} -even and \mathcal{CP} -odd couplings. Taking into account the relative enhancement of the pure \mathcal{CP} -odd coupling due to loop effects (see Eq. (3)), the

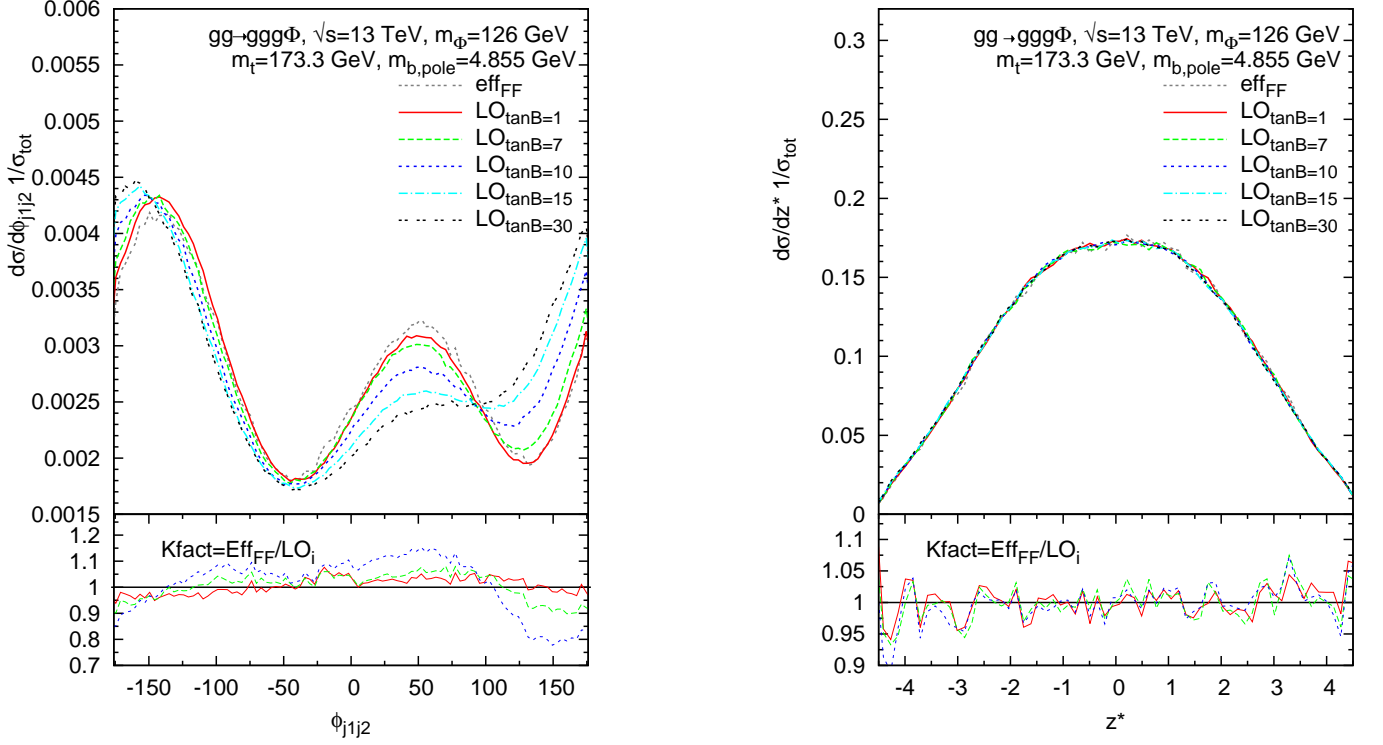


FIG. 5: Left: azimuthal angle correlation ϕ_{j1j2} of the two harder jets with applied ICphi cuts of Eq. (11). Right: z^* , the normalized centralized rapidity distribution of the third jet w.r.t. the tagging jets using the VBF cuts of Eq. (13). Further, details are described in Fig. 3 and in the text.

phase shift angle is given by [15],

$$\tan \alpha = \frac{3}{2} \frac{\tilde{y}_q}{y_q}. \quad (12)$$

In our toy model scenario, Eq. (10), we assume $y_q = 3/2\tilde{y}_q$, and hence, the minima are shifted to $\alpha = 45^\circ, 135^\circ$ degrees. This can be seen in Figure 5, where we simulate effects of a general \mathcal{CP} -violating Higgs sector at the LHC for a set of different $\tan\beta$ values, illustrated with the help of the normalized ϕ_{jj} -distributions. The effective theory approximation reproduces accurately the shape of the ϕ_{jj} distribution. Whereas in the full theory, the azimuthal angle distributions receives kinematical distortions which are caused by kinematical effects due to both, the balance of the transverse momentum of the jets and the Higgs boson, and the softer momentum spectrum of the jets and the Higgs boson for high values of $\tan\beta$ (Fig.3 and 4) where bottom loop contributions dominate. Using typical vector fusion cuts,

$$m_{j1j2} > 600 \text{ GeV}, \quad |y_{j1} - y_{j2}| > 4, \quad y_{j1} \cdot y_{j2} < 0, \quad (13)$$

we show the normalized centralized rapidity distribution of the third jet with respect to the tagging jets, $z^* = (y_3 - 1/2(y_1 + y_2))/|y_1 - y_2|$. This variable reflects the nature of VBF processes involving the fusion of electro-weak Gauge bosons. In EW Hjjj production [40],

one can clearly observe how the third jet tends to accompany one of the leading jets appearing at $1/2$ and $-1/2$ respectively. Additionally, due to its color singlet nature, there is almost no jet activity in the rapidity gap region (minimum at $z^* = 0$) between the two leading tagging jets. In our case, it shows the typical behavior of a QCD induced process, and the rapidity gap between the two jets is filled up by at least a third jet due to additional gluon radiation. Furthermore, the z^* -distribution is insensitive to the change of the Higgs couplings to fermions by the model parameter $\tan\beta$.

IV. SUMMARY

In this letter, we have presented first results for the gluon fusion loop-induced sub-process $gg \rightarrow ggg\Phi$ at the LHC, where Φ corresponds to a general \mathcal{CP} -violating Higgs boson. Interference effects between loops with top- and bottom-quarks as well as between \mathcal{CP} -even and \mathcal{CP} -odd couplings of the heavy quarks were fully taken into account.

The stability of the numerical results is guaranteed by a suitable application of Ward identities and quadruple precision, which are adequate even for bottom dominated configurations.

Using a toy model scenario, we have presented effects of bottom-quark loop contributions which can lead to

visible distortions in the differential distributions of important observables for large values of $\tan\beta$.

Operating at a center of mass energy of $\sqrt{s} = 13$ TeV, for small values of $\tan\beta$, up to Higgs masses of 290 GeV and for small transverse momenta $p_T^{\text{max}} \lesssim 290$ GeV, the effective Lagrangian approximation including the form factor correction gives accurate results and can be used as a numerically fast alternative for phenomenological studies. No restriction was found in the validity of the invariant mass of the dijet system of the leading jets (not shown) for small values of $\tan\beta$. The shape of the azimuthal angle distribution is well described by the effective theory. However, distortions in the shape appear for increasing values of $\tan\beta$. A detailed description of the full process will be given in a forthcoming publication. This process will be made publicly available as part of

the VBFNLO program.

ACKNOWLEDGMENTS

It is a pleasure to thank Dieter Zeppenfeld for fruitful discussions during the development of this project. We acknowledge the support from the Deutsche Forschungsgemeinschaft via the Sonderforschungsbereich/Transregio SFB/TR-9 Computational Particle Physics. FC is funded by a Marie Curie fellowship (PIEF-GA-2011-298960) and partially by MINECO (FPA2011-23596) and by LHCPHENONET (PITN-GA-2010-264564). MK acknowledges support by the Grid Cluster of the RWTH-Aachen.

-
- [1] T. Plehn, D. L. Rainwater, and D. Zeppenfeld, *Phys.Rev.Lett.* **88**, 051801 (2002), hep-ph/0105325.
 - [2] A. Djouadi, *Phys.Rept.* **457**, 1 (2008), hep-ph/0503172.
 - [3] A. Djouadi, *Phys.Rept.* **459**, 1 (2008), hep-ph/0503173.
 - [4] B. E. Cox, J. R. Forshaw, and A. D. Pilkington, *Phys.Lett.* **B696**, 87 (2011), 1006.0986.
 - [5] B. Coleppa, K. Kumar, and H. E. Logan, *Phys.Rev.* **D86**, 075022 (2012), 1208.2692.
 - [6] A. Freitas and P. Schwaller, *Phys.Rev.* **D87**, 055014 (2013), 1211.1980.
 - [7] C. Englert, M. Spannowsky, and M. Takeuchi, *JHEP* **1206**, 108 (2012), 1203.5788.
 - [8] R. V. Harlander and T. Neumann, *Phys.Rev.* **D88**, 074015 (2013), 1308.2225.
 - [9] W.-F. Chang, W.-P. Pan, and F. Xu, *Phys.Rev.* **D88**, 033004 (2013), 1303.7035.
 - [10] A. Djouadi and G. Moreau, (2013), 1303.6591.
 - [11] ATLAS Collaboration, G. Aad *et al.*, *Phys.Lett.* **B716**, 1 (2012), 1207.7214.
 - [12] S. Chatrchyan *et al.*, *Phys. Lett. B* **716**, 30 (2012).
 - [13] V. Del Duca, W. Kilgore, C. Oleari, C. Schmidt, and D. Zeppenfeld, *Phys.Rev.Lett.* **87**, 122001 (2001), hep-ph/0105129.
 - [14] K. Odagiri, *JHEP* **0303**, 009 (2003), hep-ph/0212215.
 - [15] V. Hankele, G. Klamke, D. Zeppenfeld, and T. Figy, *Phys.Rev.* **D74**, 095001 (2006), hep-ph/0609075.
 - [16] G. Klamke and D. Zeppenfeld, *JHEP* **0704**, 052 (2007).
 - [17] K. Hagiwara, Q. Li, and K. Mawatari, *JHEP* **0907**, 101 (2009), 0905.4314.
 - [18] F. Campanario, M. Kubocz, and D. Zeppenfeld, *Phys.Rev.* **D84**, 095025 (2011), 1011.3819.
 - [19] V. Del Duca *et al.*, *JHEP* **0610**, 016 (2006).
 - [20] V. Del Duca, *Acta Phys.Polon.* **B39**, 1549 (2008).
 - [21] J. R. Andersen, K. Arnold, and D. Zeppenfeld, *JHEP* **1006**, 091 (2010), 1001.3822.
 - [22] J. M. Campbell, R. K. Ellis, and G. Zanderighi, *JHEP* **0610**, 028 (2006), hep-ph/0608194.
 - [23] H. van Deurzen *et al.*, *Phys.Lett.* **B721**, 74 (2013), 1301.0493.
 - [24] F. Campanario and M. Kubocz, *Phys.Rev.* **D88**, 054021 (2013), 1306.1830.
 - [25] G. Cullen *et al.*, *Phys.Rev.Lett.* **111**, 131801 (2013), 1307.4737.
 - [26] K. Arnold *et al.*, *Comput.Phys.Comm.* **180**, 1661 (2009), 0811.4559.
K. Arnold *et al.*, (2011), 1107.4038.
K. Arnold *et al.*, (2012), 1207.4975.
 - [27] K. Hagiwara and D. Zeppenfeld, *Nucl.Phys.* **B274**, 1 (1986).
 - [28] K. Hagiwara and D. Zeppenfeld, *Nucl.Phys.* **B313**, 560 (1989).
 - [29] F. Campanario, *JHEP* **1110**, 070 (2011), 1105.0920.
 - [30] G. Passarino and M. Veltman, *Nucl.Phys.* **B160**, 151 (1979).
 - [31] A. Denner and S. Dittmaier, *Nucl.Phys.* **B734**, 62 (2006), hep-ph/0509141.
 - [32] G. 't Hooft and M. Veltman, *Nucl.Phys.* **B153**, 365 (1979).
 - [33] A. Denner, U. Nierste, and R. Scharf, *Nucl.Phys.* **B367**, 637 (1991).
 - [34] J. Alwall *et al.*, *JHEP* **0709**, 028 (2007), 0706.2334.
 - [35] J. Alwall, M. Herquet, F. Maltoni, O. Mattelaer, and T. Stelzer, *JHEP* **1106**, 128 (2011), 1106.0522.
 - [36] F. Campanario, Q. Li, M. Rauch, and M. Spira, (2012), 1211.5429.
 - [37] J. Pumplin *et al.*, *JHEP* **0207**, 012 (2002).
 - [38] M. Spira, *Fortsch.Phys.* **46**, 203 (1998), hep-ph/9705337.
 - [39] J. Vermaseren, S. Larin, and T. van Ritbergen, *Phys.Lett.* **B405**, 327 (1997), hep-ph/9703284.
 - [40] F. Campanario, T. Figy, S. Platzer, and M. Sjodahl, *Phys.Rev.Lett.* **111**, 211802 (2013), 1308.2932.